



This is a repository copy of *Efficient occlusion of nanoparticles within inorganic single crystals*.

White Rose Research Online URL for this paper:
<https://eprints.whiterose.ac.uk/163313/>

Version: Accepted Version

Article:

Ning, Y. and Armes, S.P. orcid.org/0000-0002-8289-6351 (2020) Efficient occlusion of nanoparticles within inorganic single crystals. *Accounts of Chemical Research*, 53 (6). pp. 1176-1186. ISSN 0001-4842

<https://doi.org/10.1021/acs.accounts.0c00103>

This document is the Accepted Manuscript version of a Published Work that appeared in final form in *Accounts of Chemical Research*, copyright © American Chemical Society after peer review and technical editing by the publisher. To access the final edited and published work see <https://doi.org/10.1021/acs.accounts.0c00103>

Reuse

Items deposited in White Rose Research Online are protected by copyright, with all rights reserved unless indicated otherwise. They may be downloaded and/or printed for private study, or other acts as permitted by national copyright laws. The publisher or other rights holders may allow further reproduction and re-use of the full text version. This is indicated by the licence information on the White Rose Research Online record for the item.

Takedown

If you consider content in White Rose Research Online to be in breach of UK law, please notify us by emailing eprints@whiterose.ac.uk including the URL of the record and the reason for the withdrawal request.



eprints@whiterose.ac.uk
<https://eprints.whiterose.ac.uk/>

Efficient Occlusion of Nanoparticles within Inorganic Single Crystals

Yin Ning* and Steven P. Armes*

Department of Chemistry, University of Sheffield, Brook Hill, Sheffield, South Yorkshire, S3
7HF, U.K.

CONSPECTUS (400-500 words): In principle, the incorporation of guest nanoparticles within host crystals should provide a straightforward and versatile route to a wide range of nanocomposite materials. However, crystallization normally involves expelling impurities so nanoparticle occlusion is both counter-intuitive and technically challenging. Clearly, the nanoparticles should have a strong interaction with the growing crystalline lattice, but quantifying such affinity has been challenging; the basic principles that govern efficient nanoparticle occlusion within inorganic single crystals are rather poorly understood. In the past few years we have focused on the elucidation of robust design rules for such systems; our progress is summarized in this article.

Polymerization-induced self-assembly (PISA) is widely recognized as a powerful platform technology for the preparation of a broad range of model organic nanoparticles. Herein PISA was exploited to prepare sterically-stabilized diblock copolymer nano-objects (e.g. spheres, worms or

vesicles) of varying size using steric stabilizers of well-defined chain length, variable anionic charge density, tunable surface density and adjustable chemical functionality (e.g. carboxylic acid, phosphate, sulfate or sulfonate groups). Thus we were able to systematically investigate how such structural parameters influence nanoparticle occlusion. Given its commercial importance for many industrial sectors, calcium carbonate was selected as the model host crystal for nanoparticle occlusion studies. Perhaps surprisingly, the extent of nanoparticle occlusion is not particularly sensitive to nanoparticle size or morphology. However, the steric stabilizer chain length can play a key role: relatively short chains lead to surface-confined occlusion, while sufficiently long chains enable uniform nanoparticle occlusion to be achieved throughout the crystal lattice (albeit sometimes inducing a significant change in crystal morphology). Optimizing the anionic charge density and surface density of the stabilizer chains is required to maximize the extent of nanoparticle occlusion, while steric stabilizer chains comprising anionic carboxylate groups led to greater occlusion compared to those composed of phosphate, sulfate, or sulfonate groups.

Subsequently, our occlusion studies were extended to include functional hybrid nanocomposite crystals. For example, the spatially-controlled occlusion of poly(glycerol monomethacrylate)-stabilized gold nanoparticles was achieved within semiconductive ZnO crystals by either controlling the nanoparticle concentration or by delaying their addition to the reaction mixture. Moreover, oil droplets of up to 500 nm have been incorporated into calcite crystals at up to 11% by mass, despite the large mismatch in surface energy between the hydrophobic oil droplets and the ionic crystal lattice. We have also explored a ‘Trojan horse’ strategy, whereby cargos comprising nanoparticles or soluble dye molecules are first encapsulated within anionic block copolymer vesicles prior to their incorporation within calcite crystals. This approach offers a generic and efficient strategy for the occlusion of many types of guest species

into single crystals. In summary, we have established important guidelines for efficient nanoparticle occlusion within crystals, which opens up new avenues for the synthesis of next-generation hybrid materials.

1. INTRODUCTION

Biomaterials are typically composed of organic additives embedded within an inorganic matrix.¹ Remarkable improvements in mechanical properties can be achieved even with relatively low levels of organic additives.² Therefore, scientists have sought a fundamental understanding of biomineralization with the aim of mimicking this strategy for the design of next-generation nanocomposite materials.³⁻⁶

The interaction of *water-soluble polymers* with growing crystals is well-known and has been intensively studied.⁷ However, the efficient uniform occlusion of *nanoparticles* within inorganic crystals is a formidable technical challenge. Indeed, examples of either unsuccessful or non-uniform nanoparticle occlusion have been reported by various research teams.⁸⁻¹⁰ Often, only surface-confined occlusion is achieved, i.e. the nanoparticles merely decorate the crystal surface. Wegner and co-workers first reported the incorporation of latex particles into ZnO or calcite crystals.¹¹⁻¹³ Subsequently, Kim et al. occluded commercial latexes¹⁴ and anionic diblock copolymer micelles¹⁵ within calcite single crystals and showed that such nanocomposites exhibit enhanced hardness compared to calcite of geological origin. Notably, there are more examples demonstrating guest species occlusion can improve mechanical properties,¹⁶ tune the band gap of the semiconductor¹⁷ and enhance the charge-transfer properties.¹⁸ Kulak et al. demonstrated that polymer-modified magnetite nanoparticles could also be incorporated into ZnO.¹⁹ Huo and co-workers occluded various poly(*N*-vinyl pyrrolidone)-stabilized inorganic nanoparticles (e.g. Au, Pt, Fe₃O₄ and CdTe nanoparticles, NaYF₄ rods, etc.) within metal-organic frameworks (MOFs).²⁰ Such nanocomposites can exhibit enhanced catalytic, magnetic or optical properties conferred by the nanoparticles while retaining beneficial MOF properties such as molecular sieving. Clearly, efficient occlusion of functional guest nanoparticles within host crystals enables the design of a

wide range of hybrid materials that exhibit a desirable combination of properties which cannot be accessed using the individual components alone.²¹⁻²²

Nevertheless, progress in this field has relied mainly on empirical trial-and-error experiments, owing to a lack of fundamental knowledge regarding the critical parameters that govern efficient nanoparticle occlusion within inorganic crystals. Herein, we summarize our recent progress in the elucidation of such design rules, particularly for nanoparticle occlusion within calcium carbonate crystals grown using the ammonia diffusion method.

2. RATIONAL DESIGN OF MODEL NANOPARTICLES USING POLYMERIZATION-INDUCED SELF-ASSEMBLY

Elucidating the design rules for nanoparticle occlusion within inorganic crystals requires the precision synthesis of model nanoparticles. We elected to use reversible addition-fragmentation chain transfer polymerization (RAFT) polymerization, which enables the synthesis of well-defined diblock copolymer chains with relatively narrow molecular weight distributions ($M_w/M_n < 1.30$). In particular, RAFT-mediated PISA provides a convenient and highly versatile synthetic route to diblock copolymer nanoparticles at up to 50 wt.% solids.²³ Moreover, this approach is generic: it is applicable to a wide range of functional vinyl monomers and can be conducted in water, alcoholic media or non-polar solvents. PISA involves growing an insoluble block from a soluble precursor or macromolecular chain transfer agent (macro-CTA): when the growing second block reaches a certain critical degree of polymerization (DP) this induces micellar nucleation. The final diblock copolymer morphology can be either spheres, worms or vesicles depending on the relative volume fractions of the two blocks (see **Figure 1**). The soluble precursor acts as the steric stabilizer while the insoluble block forms the nanoparticle cores (or membrane, in the case of vesicles).

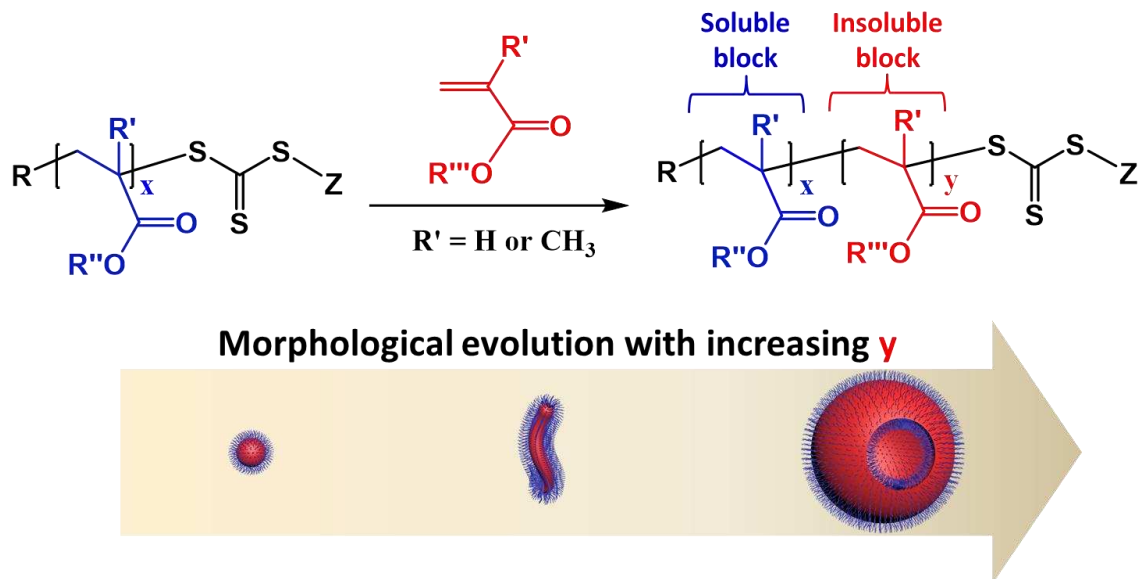


Figure 1. Basic principle of polymerization-induced self-assembly (PISA) using reversible addition-fragmentation chain transfer (RAFT) polymerization, which involves the use of an organosulfur-based chain transfer agent (in this case a trithiocarbonate). The schematic cartoon illustrates the morphological evolution that can occur when the mean degree of polymerization (DP) of the insoluble red block is systematically increased when using a blue steric stabilizer of constant DP.

3. PARAMETERS THAT GOVERN NANOPARTICLE OCCLUSION WITHIN CALCITE SINGLE CRYSTALS

Crystallization is a complex process that can occur under various conditions. In this Account, we focus on the parameters that govern the extent of occlusion of guest nanoparticles within host crystals. Thus only the structural parameters associated with the model nanoparticles were systematically examined while the crystallization conditions (e.g. crystal precursor concentration, crystallization rate, temperature, etc.) were kept constant.

It is emphasized that the guest nanoparticles do not act as *nuclei* for growth of the host crystals. Instead, the nanoparticles adsorb onto the growing crystal surface and subsequently become engulfed by the advancing steps. Both De Yoreo and co-workers²⁴ and Estroff and co-workers²⁵ have gained important insights into the mechanism of nanoparticle occlusion within calcite by

performing *in situ* atomic force microscopy (AFM) studies. There are three types of interactions between guest nanoparticles and the growing crystal surface: (i) reversible nanoparticle attachment, (ii) nanoparticle ‘hovering’ while the growing steps pass underneath, and (iii) engulfment of adsorbed nanoparticles by the advancing steps. Moreover, *in situ* AFM was also used by Zhong et al. to study the dislocation generation by particle incorporation.²⁶⁻²⁷

3.1. Morphology and Size

So far as we are aware, nanoparticle morphology (symmetric spheres, vesicles or asymmetric worms) and size (from 5 nm to 500 nm) do not appear to affect occlusion within calcite crystals. For example, poly(methacrylic acid)₇₃-poly(benzyl methacrylate)₂₀₀ [M₇₃-B₂₀₀] diblock copolymer nanoparticles can be prepared by RAFT-mediated PISA in either methanol/water or methanol/ethanol mixtures (see **Figure 2a**).²⁸ In the former case, only kinetically-trapped spheres are formed owing to the anionic character of the ionized poly(methacrylic acid)₇₃ stabilizer chains, which prevent sphere-sphere fusion. In contrast, well-defined vesicles are produced when using a methanol/ethanol mixture. Nevertheless, uniform occlusion was achieved for both types of diblock copolymer nanoparticles (see **Figure 2**). Moreover, highly asymmetric M₇₁-B₉₈ diblock copolymer worms can also be efficiently incorporated within calcite.²⁹ Thus occlusion appears to be surprisingly insensitive to the nanoparticle morphology.

To date, a wide range of nanoparticles, including polymer latexes,¹⁴ polymer-stabilized inorganic nanoparticles,³⁰⁻³⁴ sterically-stabilized diblock copolymer nano-objects (e.g. spheres,³⁵⁻³⁷ worms²⁹ or vesicles³⁸⁻³⁹), block copolymer-stabilized oil droplets,⁴⁰ and soil-derived organic matter⁴¹ have been examined in the context of calcite occlusion. The mean particle size ranges from 5 nm to 500 nm, which indicates nanoparticle size does not affect their occlusion within calcite crystals in this investigated range. Intuitively, there is likely to be an upper limit particle size beyond which occlusion becomes negligible. It is perhaps also worth bearing in mind that any upper limit guest size is likely to depend on the intrinsic dimensions of the host crystals. For example, calcite typically forms relatively large crystals of around 20-40 μm ,⁴⁰ whereas ZnO crystals are usually of the order of 1 μm or less.^{32, 35}

3.2. Steric Stabilizer Chain Length

Clearly, the surface chemistry of the guest nanoparticles plays a key role in dictating their interaction with the growing surface of the host crystals. Moreover, surface chemistry is also critical for the nanoparticles to maintain colloidal stability under the chosen occlusion conditions, which may include elevated temperature¹⁹, variation in pH or the presence of divalent cations (e.g. Ca^{2+} or Zn^{2+}).³²

PISA is a powerful platform technology that provides excellent control over the mean length of the steric stabilizer chains within diblock copolymer nanoparticles by simply varying the DP of the soluble precursor block (or macro-CTA). For example, a series of four $M_x\text{-}B_y$ diblock copolymer nanoparticles were prepared via RAFT dispersion polymerization of benzyl methacrylate. The poly(methacrylic acid) stabilizer DP (or x) was either 29 or 73 (see **Figure 2a**). Depending on the solvent medium, either a spherical or a vesicular morphology could be obtained. Small angle x-ray scattering (SAXS) enables rigorous structural analysis of these nanoparticles in terms of their morphology, particle size, mean aggregation number, surface density of stabilizer chains (i.e. the mean number of copolymer chains per unit surface area) and vesicle membrane thickness.²⁸ Such nanoparticles are sufficiently large to determine their spatial distribution within calcite crystals using established imaging techniques such as transmission electron microscopy (TEM),¹⁵ scanning electron microscopy (SEM),³⁷⁻³⁸ confocal laser scanning microscopy (CLSM),³⁹⁻⁴⁰ or ptychographic x-ray tomography.⁴²

Calcite crystals precipitated in the presence of these four model nanoparticles were fractured prior to SEM studies, see **Figures 2b-2i**. These images indicate that surface-confined occlusion, where nanoparticles are only incorporated at the near-surface of the crystal, occurs when $M_x\text{-}B_y$ nanoparticles have relatively short steric stabilizer chains ($x = 29$). In contrast, uniform occlusion - whereby nanoparticles are evenly incorporated throughout the whole crystal - occurs when such nanoparticles possess relatively long stabilizer chains ($x = 73$). Systematic variation of the poly(methacrylic acid) chain length indicated that a minimum DP of approximately 50 is required to ensure uniform nanoparticle occlusion.²⁸ However, larger nanoparticles may require longer stabilizer chains to achieve uniform occlusion.¹⁰ In this study, these four model nanoparticles range in size from ~30 nm up to 200 nm. Clearly, neither size nor morphology can explain the observed

qualitative difference in nanoparticle occlusion. Moreover, any possible effect of surface stabilizer chain density was also excluded.²⁸ Instead, it is the steric stabilizer chain length that dictates whether surface-confined occlusion or uniform occlusion occurs within calcite crystals.

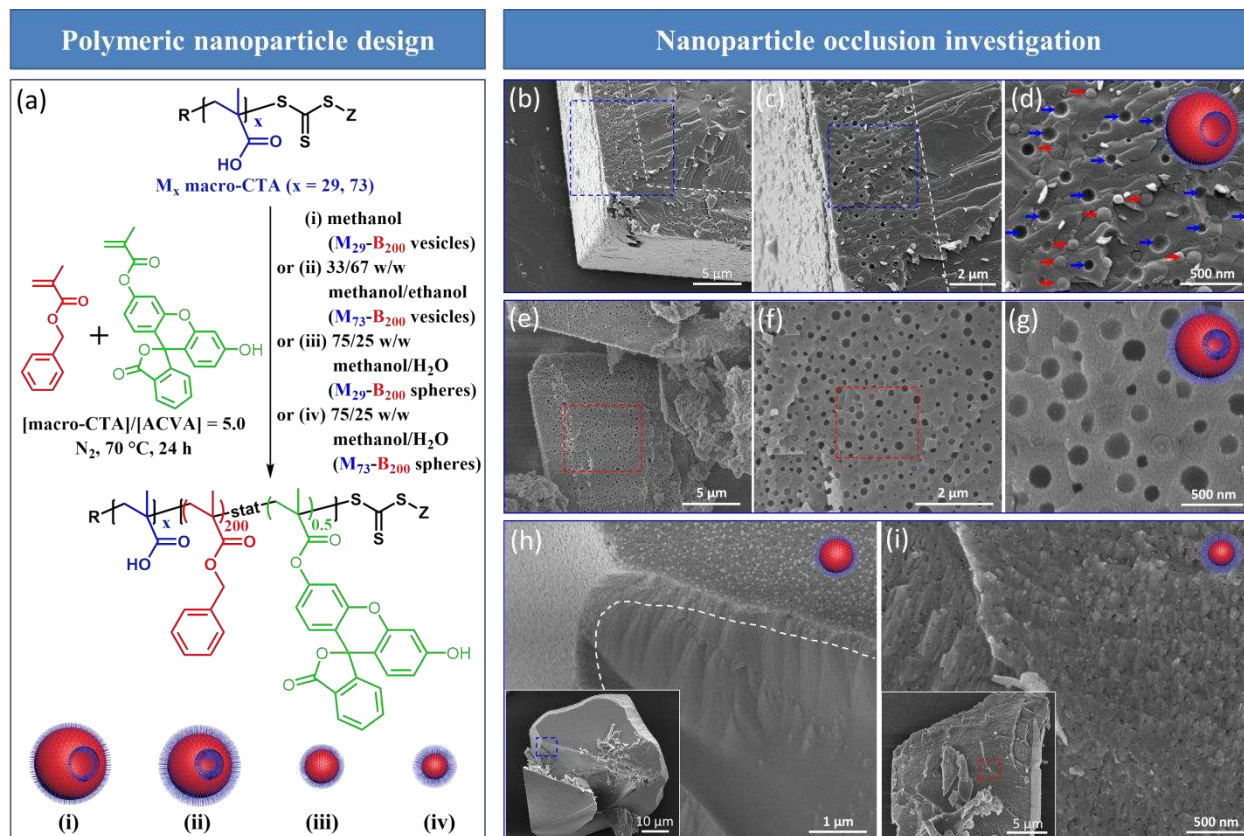


Figure 2. Effect of varying the steric stabilizer chain length on the type of nanoparticle occlusion within calcite single crystals. (a) Synthesis of fluorescein-labeled poly(methacrylic acid)_x-poly(benzyl methacrylate)_y (M_x-B_y) diblock copolymer nanoparticles via RAFT-mediated PISA, where the choice of solvent dictates the final copolymer morphology (i.e. spheres or vesicles). Representative SEM images recorded for randomly-fractured calcite crystals precipitated in the presence of (b-d) 0.1% w/w M₂₉-B₂₀₀ vesicles; (e-g) 0.1% w/w M₇₃-B₂₀₀ vesicles; (h) 0.01% w/w M₂₉-B₂₀₀ spheres; (i) 0.01% w/w M₇₃-B₂₀₀ spheres. The insets shown in (h) and (i) are the corresponding low magnification SEM images, respectively. Reproduced from ref 28. Copyright 2019 American Chemical Society.

Obviously, nanoparticles that strongly interact with the growing host crystals are more likely to be engulfed during crystal growth. In this context, nanoparticles bearing longer

poly(methacrylic acid) stabilizer chains can adopt many more conformations in order to bind to the growing calcite surface. Surface-confined occlusion suggests that nanoparticles only become incorporated within the host crystal during the latter stages of crystallization. Clearly, the concentration of divalent Ca^{2+} ions is gradually reduced during calcite formation. In principle, this results in less ionic cross-linking between anionic carboxylate groups on neighbouring poly(methacrylic acid) stabilizer chains. Thus, the stabilizer chains gain more conformational freedom, which enhances nanoparticle adsorption and belatedly promotes occlusion. Moreover, the growing calcite surface contains longer step edges and more kink sites, which should promote surface-confined occlusion in the latter stages of crystallization.²⁸ Thus this study provides an explanation for the observation of surface-confined nanoparticle occlusion within calcite, which was first noted by Lu et al. in 2005.⁸

Ideally, when designing a series of model nanoparticles to elucidate design rules, only one parameter should be varied with all others being held constant. However, there is often some unavoidable interplay between various structural parameters. For example, systematic variation of the steric stabilizer chain length leads to the formation of spherical nanoparticles of differing particle size aggregation number and surface stabilizer chain density when targeting the same DP for the core-forming block.²⁸ To address this well-known problem, we designed a series of model vesicles using a synthetic protocol inspired by the An research group.⁴³ Importantly, the vesicle membrane is covalently cross-linked, which enables the steric stabilizer chain length to be varied without altering the lumen volume (see **Figure 3**). Thus, the surface density of the anionic steric stabilizer chains remains constant as they are grown from the membranes of non-ionic precursor vesicles. Moreover, such vesicles were labeled by copolymerizing a small amount of fluorescent comonomer, which enables visualization of the occluded vesicles by fluorescent microscopy. Finally, silica nanoparticles can be readily encapsulated within such vesicles to serve as a model payload. This approach offers an attractive and versatile route for the design of a range of new hybrid materials, as well as allowing the elucidation of design rules.³⁸

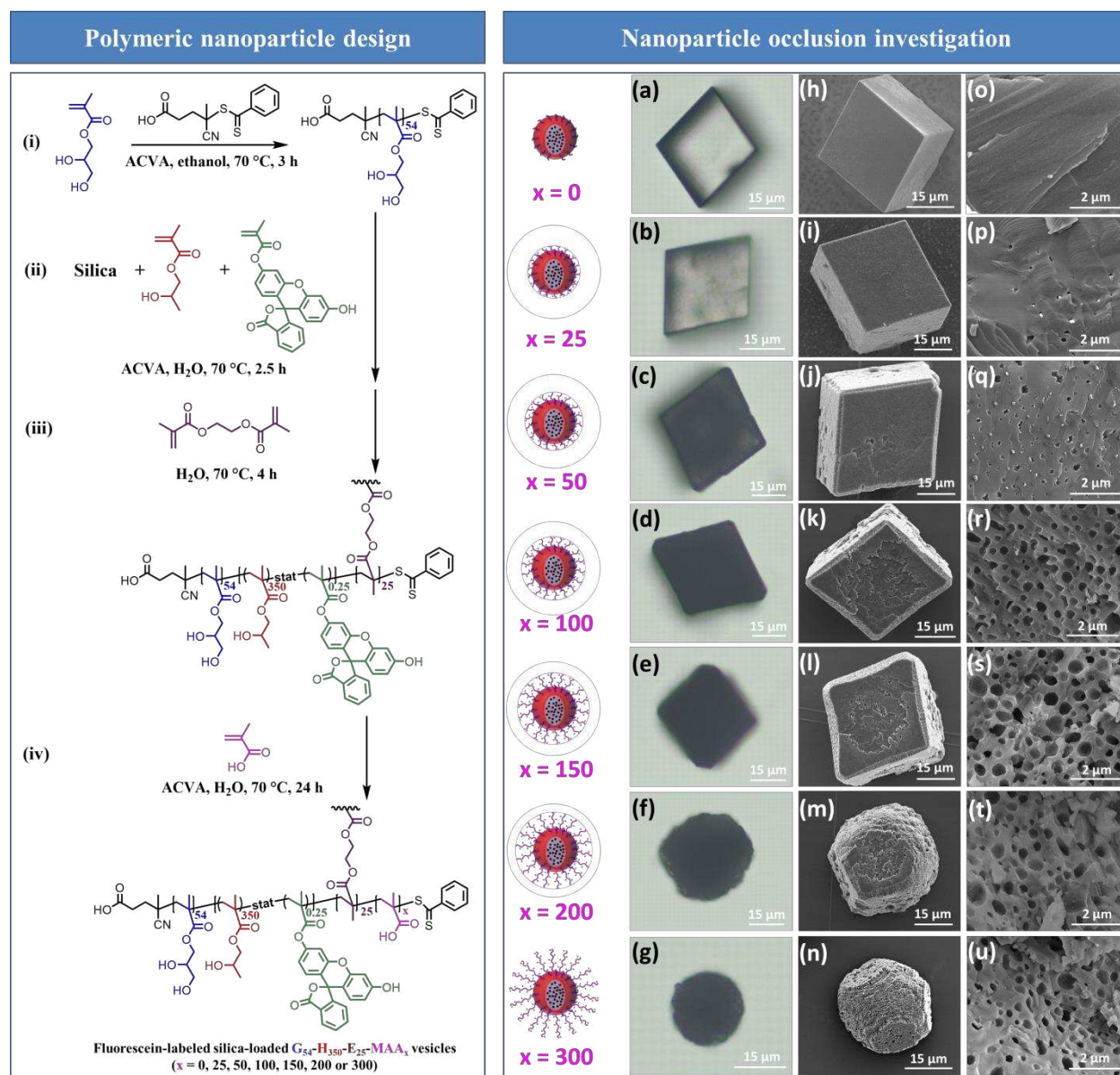


Figure 3. Effect of varying the steric stabilizer chain length on the occlusion of vesicles within calcite crystals. (i-iv) Synthesis of fluorescein-labeled silica-loaded vesicles with a fixed lumen diameter and tunable steric stabilizer chain length. Representative optical microscopy images (a-g) and SEM images (h-n) of calcite crystals grown in the presence of vesicles bearing poly(methacrylic acid) chains of varying DP. (o-u) SEM images of the corresponding fractured calcite crystals, revealing the presence of the occluded vesicles. Reproduced from ref 38. Copyright 2019 American Chemical Society.

Precise control over the poly(methacrylic acid) chain length provided an unprecedented opportunity to systematically investigate how this parameter affects the extent of nanoparticle occlusion. It turns out that the stabilizer DP plays an important role in dictating both the extent of nanoparticle occlusion and the calcite crystal morphology: sufficiently long stabilizer chains are required to achieve uniform nanoparticle occlusion, but if the stabilizer chains are too long this adversely affects the crystal morphology without increasing the extent of occlusion (see **Figures 3a-n**).³⁸ In principle, longer poly(methacrylic acid) stabilizer chains should enable stronger vesicle binding to the growing crystal surface and hence lead to higher extents of vesicle occlusion. We hypothesize that mutual electrostatic repulsion between these highly anionic vesicles may prevent their close approach during occlusion. The longer stabilizer chains have many more degrees of freedom, which enables stronger binding to the growing crystal surface and thus causes a change in the crystal morphology.

3.3. Anionic Charge Content within the Surface Stabilizer Chains

Statistically copolymerization of an anionic monomer (2-(phosphonooxy)ethyl methacrylate, **P**) with a non-ionic monomer (glycerol monomethacrylate, **G**) in various molar ratios enables the anionic charge density of the resulting steric stabilizer chains to be systematically varied, see **Figures 4a-b**. The *overall* DP of such copolymer stabilizer chains was selected to be ~50 because our previous studies showed that this is sufficiently long to ensure uniform nanoparticle occlusion.^{28, 38} Systematic variation of the anionic charge density enabled us to ask the following questions. What is the minimum number of anionic comonomer units in the steric stabilizer block required to achieve uniform nanoparticle occlusion within calcite crystals? How does varying the anionic charge density within the stabilizer chains affect the extent of nanoparticle occlusion?

SEM studies indicated that higher levels of nanoparticle occlusion can be achieved by increasing the anionic character of the steric stabilizer chains (**Figure 4c**). Fewer than 21 phosphate groups per stabilizer chain led to non-uniform occlusion while a relatively high proportion (e.g. ≥ 32 phosphate groups per chain) ensured uniform occlusion. Moreover, only *surface-confined* occlusion of poly(2-(phosphonooxy)ethyl methacrylate)₃₂-poly(benzyl methacrylate)₃₀₀ nanoparticles within calcite crystals could be achieved in an earlier study.²⁸ We tentatively suggest that incorporating non-ionic comonomer units within the steric stabilizer chains confers greater

conformational freedom while simultaneously reducing the probability of ionic cross-linking between neighboring phosphate groups within the stabilizer chains. In both cases, this should facilitate nanoparticle binding to the growing crystal surface.

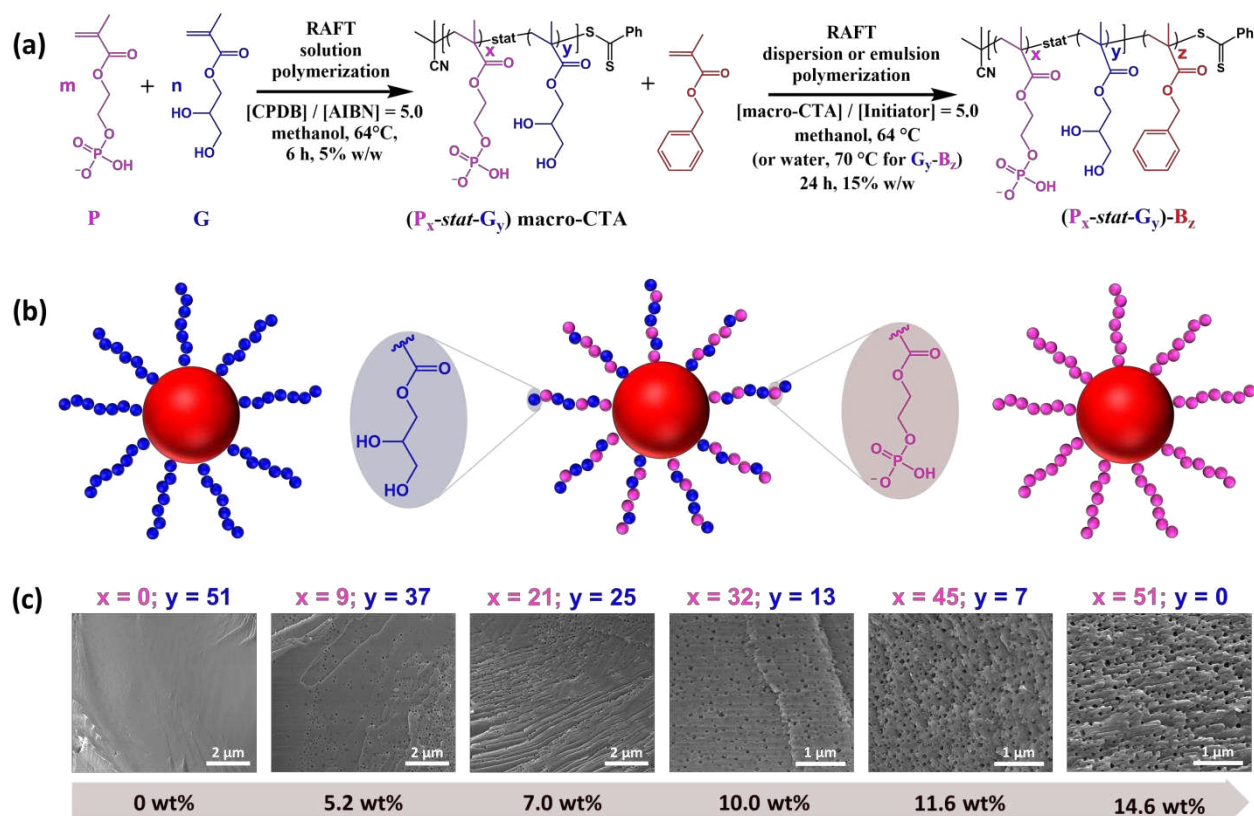


Figure 4. Effect of varying the anionic charge density within the steric stabilizer chains on nanoparticle occlusion. (a) PISA synthesis of a series of sterically-stabilized spherical nanoparticles containing a variable number of anionic phosphate groups within the stabilizer chains; (b) schematic cartoons summarizing the chemical and structural features of these copolymer nanoparticles; (c) SEM images recorded for the randomly-fractured calcite crystals grown in the presence of these anionic nanoparticles. Reproduced from ref 45. Copyright 2019 John Wiley & Sons, Inc.

3.4. Surface Stabilizer Chain Density

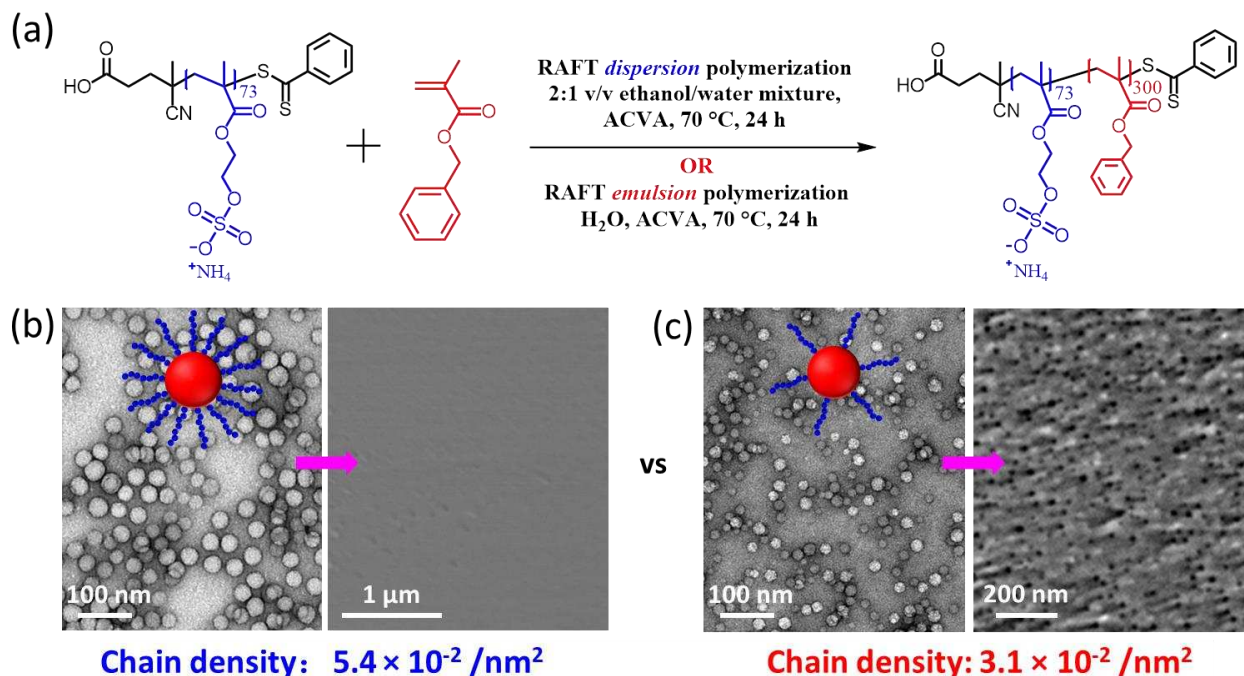


Figure 5. Effect of varying the surface density of stabilizer chains on the extent of nanoparticle occlusion within calcite crystals. (a) Synthesis of poly(ammonium 2-sulfatoethyl methacrylate)₇₃-poly(benzyl methacrylate)₃₀₀ [S₇₃-B₃₀₀] spherical nanoparticles via either RAFT dispersion polymerization or RAFT aqueous emulsion polymerization; (b) S₇₃-B₃₀₀ spheres with a relatively high density of anionic stabilizer chains and their occlusion within calcite; (c) S₇₃-B₃₀₀ spheres with a relatively low density of stabilizer chains and their occlusion within calcite. Reproduced from ref 37. Copyright 2016 American Chemical Society.

For polyelectrolytic stabilizer chains, the extent of mutual electrostatic repulsion depends on the solvent(s) selected for the PISA synthesis. A highly anionic polyelectrolyte, poly(ammonium 2-sulfatoethyl methacrylate)₇₃, was chain-extended with benzyl methacrylate in various solvent(s) with differing dielectric constants (see **Figure 5a**). The anionic stabilizer chain density should be significantly reduced when using a solvent (or solvent mixture) with a higher overall dielectric constant.³⁷ This is because greater electrostatic repulsion between neighboring polyelectrolytic chains increases their lateral inter-separation distance, which also leads to a lower mean aggregation number.

Remarkably, *lower* stabilizer chain densities lead to *higher* extents of nanoparticle occlusion. This is presumably because ionic cross-linking by Ca^{2+} ions is more likely for nanoparticles with higher stabilizer chain densities, which in turn prevents the anionic nanoparticles from interacting with the growing crystals.³⁷ In fact, an *optimum* stabilizer chain density is important for maximizing nanoparticle occlusion. This was subsequently confirmed by Kim et al., who used a binary mixture of poly(methacrylic acid) stabilizer chains to tune the anionic charge density.⁴⁴ This unexpected finding reveals an arguably counter-intuitive design rule for efficient nanoparticle occlusion within calcite crystals. Moreover, **Figure 5c** indicates such sulfate-based nanoparticles are densely distributed within the calcite crystals. Indeed, the nanoparticle concentration within such crystals is significantly higher than the original nanoparticle concentration in the reaction solution. This suggests an active uptake mechanism, which is consistent with in situ AFM studies.²⁴⁻²⁵

3.5. Surface Functionality

In general, anionic surface character appears to be important for driving nanoparticle occlusion within calcite crystals.³⁶ In this context, a wide range of anionic functionalities have been explored. Using the model cross-linked vesicle system described above, we found that anionic carboxylate groups are superior to phosphate, sulfate or sulfonate groups in promoting nanoparticle occlusion.³⁸ This is presumably because of the structural similarity between anionic carboxylate groups and CO_3^{2-} anions, which ensures intimate interaction between the nanoparticles and the calcite surface. In contrast, only very limited occlusion was observed for non-ionic poly(glycerol monomethacrylate)_x-poly(benzyl methacrylate)_y diblock copolymer nanoparticles.^{25, 37-38, 45-46} However, we serendipitously found that poly(glycerol monomethacrylate)-functionalized gold nanoparticles can be efficiently incorporated within ZnO crystals, which will be discussed in more detail in the next Section. Very recently, Kim et al. reported that such gold nanoparticles can also be densely occluded within calcite crystals and other host crystals such as calcium sulfate dihydrate and calcium oxalate monohydrate (see **Figure 6**).³³ Surprisingly, the non-ionic poly(glycerol monomethacrylate) stabilizer chains even outperform anionic poly(methacrylic acid) in terms of the extent of occlusion. In related work, Magnabosco et al. reported that 10 nm silica nanoparticles coated with a non-ionic poly(ethylene glycol)-based polymer bearing hydroxyl, amine or carboxylic acid terminal groups can be occluded within calcite, albeit with rather low

extents of occlusion.³⁴ For non-ionic polymer-coated inorganic nanoparticles, such surface modification is essential to ensure sufficient colloidal stability under the calcite growth conditions. Clearly, further work is warranted to establish whether subtle differences in the surface density of stabilizer chains might play an important role here. Alternatively, does the nature of the nanoparticle core (gold sol vs. poly(benzyl methacrylate)) influence the extent of occlusion? The latter hypothesis does not appear to be very likely but it certainly deserves to be evaluated.

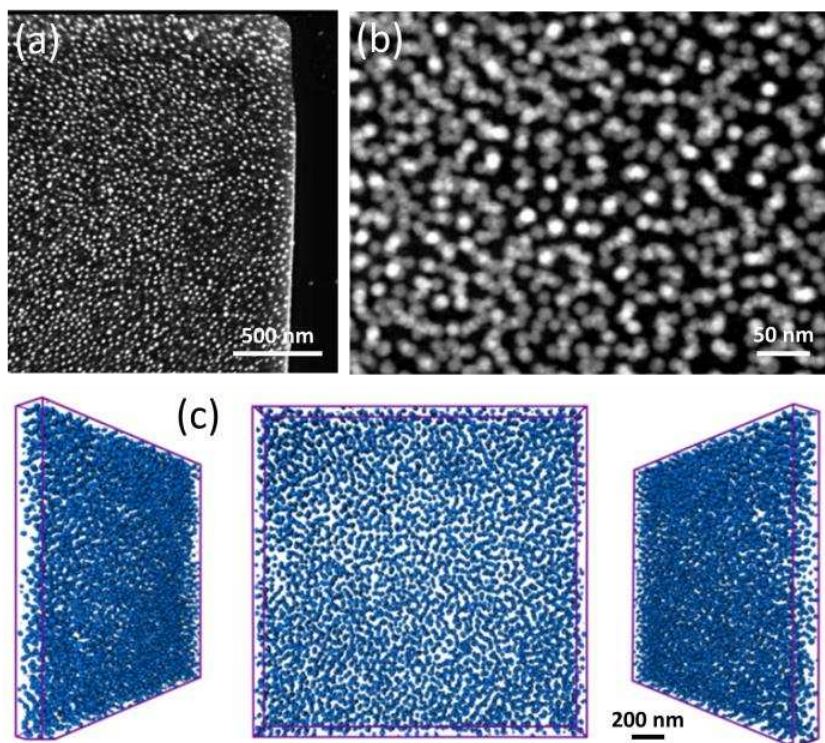


Figure 6. Calcite crystals precipitated in the presence of 0.05% w/v 14 nm poly(glycerol monomethacrylate)-functionalized gold nanoparticles. (a) SEM image of a FIB cross-section and (b) STEM HAADF image of a lamellar cut from a calcite crystal occluded with gold nanoparticles. (c) Tomographic image derived from STEM analysis showing the nanoparticle distribution within a sectioned lamella from a representative crystal. Reproduced from ref 33. Copyright 2020 Springer Nature Limited.

4. SPATIALLY CONTROLLED NANOPARTICLE OCCLUSION

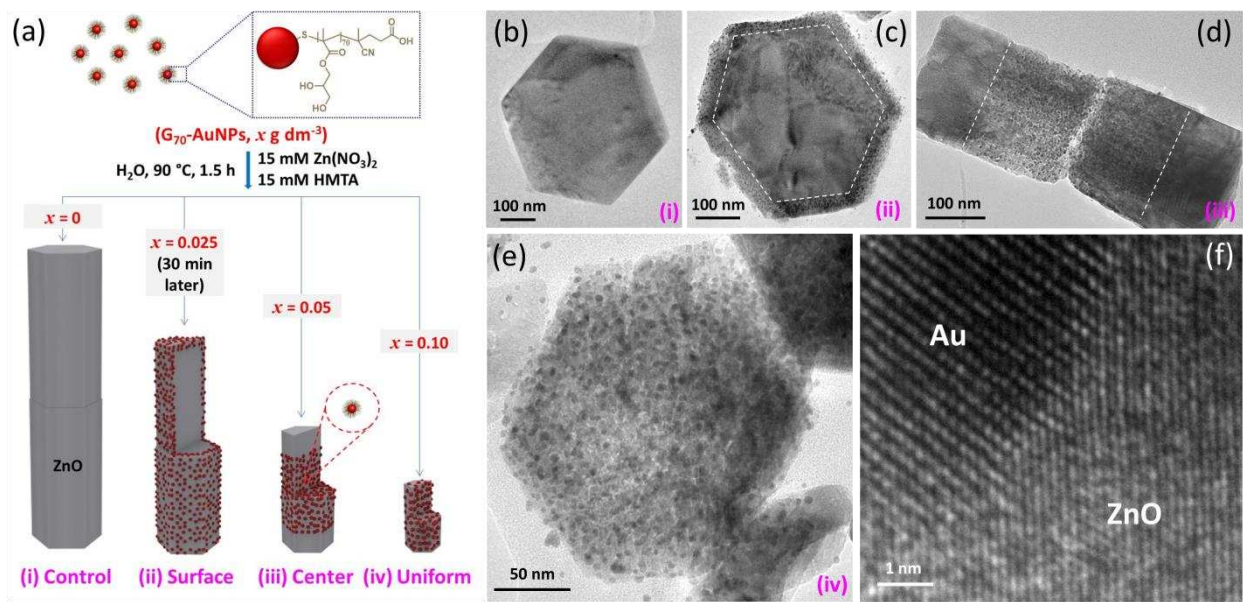


Figure 7. (a) Schematic representation of spatially-controlled occlusion of non-ionic poly(glycerol monomethacrylate)₇₀-stabilized gold nanoparticles (G₇₀-AuNPs) within ZnO crystals. Representative TEM images showing cross-sections of (b) ZnO control, (c) gold nanoparticles occluded at the near surface of ZnO crystals, (d) gold nanoparticles occluded at the center of ZnO crystals, (e) uniform occlusion of gold nanoparticles within ZnO crystals. (f) high-resolution TEM image indicating intimate contact between a single gold nanoparticle and the surrounding ZnO crystal. Reproduced from ref 32. Copyright 2019 John Wiley & Sons, Inc.

Controlling the spatial distribution of nanoparticles within host crystals is highly desirable because this may be required to optimize various physical properties. In 2015, we occluded poly(ammonium 2-sulfatoethyl methacrylate)₇₃-poly(benzyl methacrylate)₃₀₀ [S₇₃-B₃₀₀] diblock copolymer spheres within semiconductive ZnO crystals.³⁵ Unfortunately, the same protocol proved to be unsuccessful for the occlusion of poly(ammonium 2-sulfatoethyl methacrylate)-modified gold nanoparticles. However, while conducting a control experiment, we serendipitously found that non-ionic poly(glycerol monomethacrylate)-modified gold nanoparticles can be efficiently incorporated into ZnO. Moreover, the spatial distribution of such nanoparticles can be surface-confined by delaying addition of the gold nanoparticles for 30 min. Alternatively, occlusion can be restricted to just the cores of the rod-like ZnO crystals or be uniform throughout

the ZnO crystals, simply by varying the Zn^{2+} concentration (see **Figure 7**). FT-IR spectroscopy studies suggest that the pendent *cis*-diol groups on the non-ionic poly(glycerol monomethacrylate) stabilizer chains can act as a chelating ligand for the Zn^{2+} cations. Presumably, this specific interaction promotes nanoparticle adsorption at the crystal surface and hence provides the driving force for occlusion. It is well-documented that anionic macromolecules were intensively studied in the context of biomineralization while non-ionic counterparts were largely ignored.⁷ It is worth noting that nanoparticle occlusion provides a unique model system to study biomineralization.^{15, 32, 47} It seems that we may need to reconsider whether certain non-ionic biomolecules might play important roles during biomineralization.

To date, no discrete surface layer has been observed for the occluded nanoparticles, regardless of their chemical structure. Thus, it seems that the crystalline host material penetrates the steric stabilizer layer and comes into intimate contact with the nanoparticle cores.³² In principle, this could lead to emergent optical or electrical properties. In particular, uniform occlusion of gold nanoparticles within ZnO crystals did not disturb the long-range order of the host material (see **Figure 7f**). Moreover, XPS studies indicated intimate contact between the metallic gold nanocomposite cores and the semiconductive ZnO host.³² The photocatalytic properties of these Au/ZnO nanocomposites was evaluated by investigating the photodegradation of a model rhodamine B dye. The rate of dye photodegradation increases monotonically with Au content within the ZnO crystals. Thus this study suggests that enhanced properties can be achieved by combining two functional components to form nanocomposite crystals using a nanoparticle occlusion strategy.

5. A ‘TROJAN HORSE’ STRATEGY

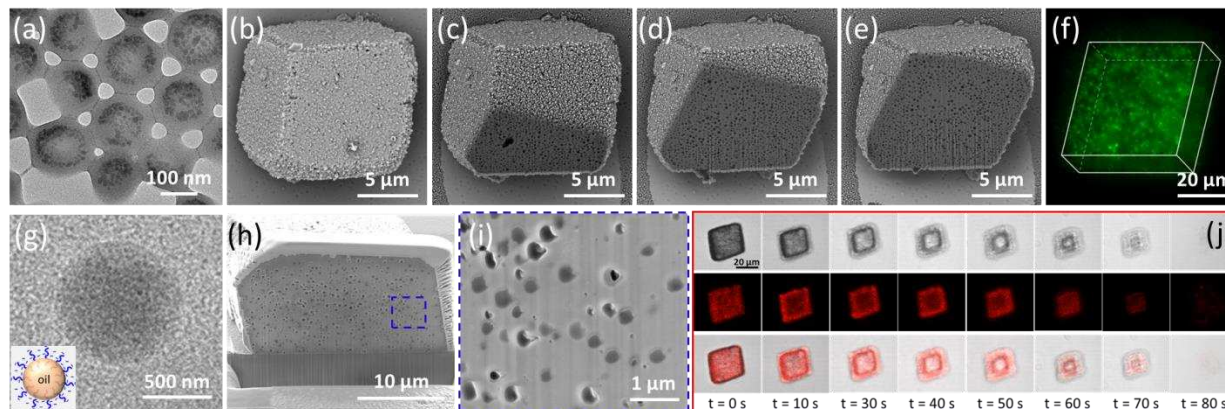


Figure 8. Various species can be occluded within calcite crystals using a ‘Trojan horse’ strategy based on anionic diblock copolymer vesicles or nanoemulsions: (a) silica-loaded M_{69} - B_{200} vesicles; (b-e) a sequence of cross-sectional SEM images recorded over time during continuous focused ion beam (FIB) etching of an individual vesicle/calcite nanocomposite crystal; (f) confocal fluorescence microscopy image recorded for a calcite crystal containing fluorescein-loaded M_{62} - B_{300} vesicles; (g) cryo-TEM image of a methyl myristate-in-water droplet, where an anionic diblock copolymer acts as a polymeric surfactant at the oil/water interface (inset shows a schematic cartoon); (h-i) SEM images recorded for a cross-sectioned calcite crystal recorded during FIB milling confirming the uniform occlusion of oil droplets; (j) *in situ* monitoring of the release of oil droplets loaded with Nile red from calcite crystals on addition of simulated gastric fluid (SGF, pH 1.2) by confocal fluorescence microscopy. Top row reproduced from ref 39. Copyright 2018 Royal Society of Chemistry. Bottom row reproduced from ref 40. Copyright 2019 Royal Society of Chemistry.

Appropriate surface chemistry is normally considered to be a prerequisite for efficient nanoparticle occlusion. For example, surface modification with a suitable polymer is usually essential for the incorporation of inorganic nanoparticles such as gold sols within host crystals. Clearly, identification of a generic route that enabled the occlusion of unmodified nanoparticles (or other species) would be highly desirable. To address this technical challenge, we designed a versatile ‘Trojan horse’ strategy. Thus, soluble small molecules (e.g. dyes) or nanoparticles are

first encapsulated within anionic diblock copolymer vesicles. Then such cargo-loaded vesicles are incorporated into calcite crystals (see **Figures 8a-e**).³⁹ In principle, this strategy allows the occlusion of any species within a host crystal. In this context, targeting a higher DP for the hydrophobic membrane-forming block leads to a thicker vesicle membrane, which may be required to retain payloads comprising soluble small molecules (see **Figure 8f**). Alternatively, nanoparticle occlusion within calcite can also be achieved by a gel-trapping method. In 2009, Li et al. reported the incorporation of agarose gel into calcite.⁴⁸ Physically trapping a range of inorganic nanoparticles (e.g. gold sols, Fe₃O₄ sols or CdTe quantum dots) within such gel networks led to their passive engulfment within this host crystalline matrix.⁴⁹⁻⁵⁰

Oil-in-water nanoemulsions can also act as ‘Trojan Horses’ to incorporate guest species into host crystals. It is well-known that most oils and inorganic crystals are mutually incompatible. Thus, the efficient incorporation of oil droplets into inorganic host crystals appears to be highly problematic. To address this formidable technical challenge, a series of strongly amphiphilic poly(methacrylic acid)-poly(*n*-alkyl methacrylate) diblock copolymers were prepared in the form of sterically-stabilized nanoparticles via PISA and subsequently evaluated as emulsifiers for various oils (e.g. methyl myristate, sunflower oil, isohexadecane etc.). First oil-in-water nanoemulsions with mean diameters ranging from 250 nm to 500 nm were prepared via high-pressure microfluidization (see **Figure 8g**). Systematic studies confirmed that both the copolymer concentration and the diblock composition affected the extent of oil droplet occlusion within calcite. Remarkably, optimized conditions produced calcite crystals that contained up to 11% oil by mass, as determined by thermogravimetric analysis. Moreover, the oil droplets underwent significant deformation during their occlusion owing to compressive forces exerted by the growing crystals (see **Figures 8h-i**).

Furthermore, we demonstrated that this protocol enables the incorporation of water-insoluble dyes or hydrophobic nanoparticles within calcite. More specifically, Nile Red dye, magnetite or gold nanoparticles were dissolved or dispersed within the oil phase followed by emulsification in the presence of the diblock copolymer surfactant to produce the cargo-loaded oil droplets. Finally, calcite precipitation in the presence of such oil droplets led to their uniform occlusion. Calcium carbonate is abundant, highly biocompatible and considered to be environmentally benign. The single crystal nature of the host ensures efficient retention of such guests at around neutral pH.

However, lowering the solution pH leads to triggered release via gradual dissolution of the calcite (see **Figure 8j**), suggesting potential controlled-release applications.⁴⁰ Alternatively, the brittle nature of the calcite crystals might enable oil release via mechanical rupture.

6. SUMMARY

Utilizing RAFT-mediated PISA as a convenient platform technology, a wide range of model nanoparticles have been designed to elucidate the essential design rules governing the efficient incorporation of various types of nanoparticles (organic, inorganic and even oil droplets) within calcite crystals. First, the steric stabilizer chain length of the guest nanoparticles plays a key role in dictating efficient occlusion: relatively long chains are required to ensure uniform nanoparticle occlusion whereas shorter chains only result in surface-confined occlusion. However, overly long chains do not promote further nanoparticle occlusion but instead change the crystal morphology. Second, optimization of both the anionic charge density and the surface density of the steric stabilizer chains is also required to maximize the extent of nanoparticle occlusion. Third, anionic stabilizer chains comprising carboxylate groups promote higher levels of nanoparticle occlusion within calcite crystals compared to those composed of phosphate, sulfate or sulfonate groups. Moreover, spatially-controlled nanoparticle occlusion can be achieved, while a ‘Trojan horse’ strategy based on the encapsulation of either nanoparticles or dye molecules within vesicles offers a generic protocol for the delivery of a wide range of guest species within host crystals.

Nanoparticle occlusion within inorganic single crystals is an emerging research field. It differs significantly from traditional chemical alloying and mechanical blending, because the former approach mixes components at the atomic scale while the latter does not lead to long-range order. Now that some of the important design rules governing nanoparticle occlusion have been established, the next step is to explore the full potential of this strategy to design a wide range of functional nanocomposite crystals that cannot be prepared by conventional methods, establish synthesis-structure-function relationships and evaluate potential applications. In addition, nanoparticle occlusion strategy also provides a unique model system to study biomineralization by designing suitable particulate additives.

AUTHOR INFORMATION

Corresponding Authors

*Y.Ning@sheffield.ac.uk

*s.p.arnes@sheffield.ac.uk

ORCID

Yin Ning: 0000-0003-1808-3513

Steven P. Armes: 0000-0002-8289-6351

Notes

The authors declare no competing financial interest.

Biographies

Yin Ning received his BEng degree in polymer materials and engineering from Ludong University and MEng degree in materials science from South China University of Technology. He then moved to the UK and obtained his PhD at the University of Sheffield, which was followed by a postdoctoral fellowship (both under the supervision of Prof. S. P. Armes). His current research interests involve polymerization-induced self-assembly and occlusion of nanoparticles within inorganic crystals.

Steven P. Armes obtained his BSc in Chemistry from the University of Bristol in 1983 and received his PhD from the same institution in 1987. After a postdoctoral fellowship at Los Alamos National Laboratory in New Mexico, he accepted a lectureship at Sussex University in 1989 and was promoted to full Professor in 2000. He moved to Sheffield University in 2004 to become a Professor of Polymer & Colloid Chemistry. He is currently the Director of the Sheffield Polymer Centre and also serves on the board of *Farapack Polymers*, a University spin-out company. He has received the 2013 RSC Tilden Prize, the 2014 RSC Interdisciplinary Prize, the 2016 DSM Materials Science Award, the 2017 ECIS-Solvay Prize, the 2017 RSC Macro Group Prize for outstanding achievement and the 2018 Royal Society Armourers and Brasiers' Company Prize. He was elected as a Fellow of the Royal Society in 2014.

ACKNOWLEDGMENTS

EPSRC (EP/P005241/1) is thanked for postdoctoral support for Y.N. and S.P.A. acknowledges an EPSRC *Established Career* Particle Technology Fellowship (EP/R003009/1).

REFERENCES

1. Meldrum, F. C.; Cölfen, H., Controlling mineral morphologies and structures in biological and synthetic systems. *Chem. Rev.* **2008**, *108*, 4332-4432.
2. Nudelman, F.; Sommerdijk, N. A., Biomineralization as an inspiration for materials chemistry. *Angew. Chem. Int. Ed.* **2012**, *51*, 6582-6596.
3. Mao, L.-B.; Gao, H.-L.; Yao, H.-B.; Liu, L.; Cölfen, H.; Liu, G.; Chen, S.-M.; Li, S.-K.; Yan, Y.-X.; Liu, Y.-Y.; Yu, S.-H., Synthetic nacre by predesigned matrix-directed mineralization. *Science* **2016**, *354*, 107-110.
4. Kosinova, A. V.; Kolybaeva, M. I.; Bezkrovnyaya, O. N.; Tkachenko, V. F.; Grishina, E. V.; Levchenko, A. N.; Puzikov, V. M.; Pritula, I. M., Structural and mechanical properties of KH₂PO₄ single crystals with embedded nanoparticles and organic molecules. *Cryst. Res. Technol.* **2014**, *49*, 965-974.
5. Pritula, I. M.; Kosinova, A. V.; Kolybaeva, M. I.; Bezkrovnyaya, O. N.; Grebenev, V. V.; Voloshin, A. E.; Vorontsov, D. A.; Sofronov, D. S.; Vovk, O. M.; Baumer, V. N., Some characteristic features of formation of composite material based on KDP single crystal with incorporated Al₂O₃·nH₂O nanoparticles. *Cryst. Res. Technol.* **2014**, *49*, 345-352.
6. Pritula, I. M.; Kosinova, A. V.; Vorontsov, D. A.; Kolybaeva, M. I.; Bezkrovnyaya, O. N.; Tkachenko, V. F.; Vovk, O. M.; Grishina, E. V., Peculiarities of the growth of KDP single crystals with incorporated aluminium oxyhydroxide nanoparticles. *J. Cryst. Growth* **2012**, *355*, 26-32.
7. Shtukenberg, A. G.; Ward, M. D.; Kahr, B., Crystal Growth with Macromolecular Additives. *Chem. Rev.* **2017**, *117*, 14042-14090.
8. Lu, C.; Qi, L.; Cong, H.; Wang, X.; Yang, J.; Yang, L.; Zhang, D.; Ma, J.; Cao, W., Synthesis of Calcite Single Crystals with Porous Surface by Templating of Polymer Latex Particles. *Chem. Mater.* **2005**, *17*, 5218-5224.
9. Hanisch, A.; Yang, P.; Kulak, A. N.; Fielding, L. A.; Meldrum, F. C.; Armes, S. P., Phosphonic Acid-Functionalized Diblock Copolymer Nano-Objects via Polymerization-Induced Self-Assembly: Synthesis, Characterization, and Occlusion into Calcite Crystals. *Macromolecules* **2015**, *49*, 192-204.
10. Yu, L.; Zhang, Y.; Dai, X.; Zhang, L.; Tan, J., Monodisperse poly (methyl methacrylate) microspheres with tunable carboxyl groups on the surface obtained by photoinitiated RAFT dispersion polymerization. *Chem. Commun.* **2019**, *55*, 7848-7851.
11. Wegner, G.; Baum, P.; Müller, M.; Norwig, J.; Landfester, K., Polymers designed to control nucleation and growth of inorganic crystals from aqueous media. *Macromol. Symp.* **2001**, *175*, 349-356.
12. Muñoz - Espí, R.; Qi, Y.; Lieberwirth, I.; Gomez, C. M.; Wegner, G., Surface - Functionalized Latex Particles as Controlling Agents for the Mineralization of Zinc Oxide in Aqueous Medium. *Chem. Eur. J.* **2006**, *12*, 118-129.
13. Wegner, G.; Demir, M. M.; Faatz, M.; Gorna, K.; Muñoz-Espí, R.; Guillemet, B.; Gröhn, F., Polymers and inorganics: a happy marriage? *Macromol. Res.* **2007**, *15*, 95-99.
14. Kim, Y. Y.; Ribeiro, L.; Maillot, F.; Ward, O.; Eichhorn, S. J.; Meldrum, F. C., Bio - Inspired Synthesis and Mechanical Properties of Calcite - Polymer Particle Composites. *Adv. Mater.* **2010**, *22*, 2082-2086.
15. Kim, Y.-Y.; Ganesan, K.; Yang, P.; Kulak, A. N.; Borukhin, S.; Pechook, S.; Ribeiro, L.; Kröger, R.; Eichhorn, S. J.; Armes, S. P.; Pokroy, B.; Meldrum, F. C., An artificial biomineral formed by incorporation of copolymer micelles in calcite crystals. *Nat. Mater.* **2011**, *10*, 890-896.

16. Liu, Y.; He, K.; Yuan, W.; Jin, X.; Liang, T.; Wang, Y.; Xin, H. L.; Chen, H.; Gao, C.; Li, H., Visualizing the toughening origins of gel-grown calcite single-crystal composites. *Chin. Chem. Lett.* **2018**, *29*, 1666-1670.
17. Brif, A.; Ankonina, G.; Drathen, C.; Pokroy, B., Bio-Inspired Band Gap Engineering of Zinc Oxide by Intracrystalline Incorporation of Amino Acids. *Adv. Mater.* **2014**, *26*, 477-481.
18. Ren, J.; Niu, M.; Guo, X.; Liu, Y.; Yang, X.; Chen, M.; Hao, X.; Zhu, Y.; Chen, H.; Li, H., Bulk-Heterojunction with Long-Range Ordering: C60 Single-Crystal with Incorporated Conjugated Polymer Networks. *J. Am. Chem. Soc.* **2020**, *142*, 1630-1635.
19. Kulak, A. N.; Grimes, R.; Kim, Y.-Y.; Semsarilar, M.; Anduix-Canto, C.; Cespedes, O.; Armes, S. P.; Meldrum, F. C., Polymer-Directed Assembly of Single Crystal Zinc Oxide/Magnetite Nanocomposites under Atmospheric and Hydrothermal Conditions. *Chem. Mater.* **2016**, *28*, 7528-7536.
20. Lu, G.; Li, S.; Guo, Z.; Farha, O. K.; Hauser, B. G.; Qi, X.; Wang, Y.; Wang, X.; Han, S.; Liu, X., Imparting functionality to a metal-organic framework material by controlled nanoparticle encapsulation. *Nat. Chem.* **2012**, *4*, 310.
21. Ning, Z.; Gong, X.; Comin, R.; Walters, G.; Fan, F.; Voznyy, O.; Yassitepe, E.; Buin, A.; Hoogland, S.; Sargent, E. H., Quantum-dot-in-perovskite solids. *Nature* **2015**, *523*, 324-328.
22. Tang, F.; Wang, L.; Walle, M. D.; Mustapha, A.; Liu, Y.-N., An alloy chemistry strategy to tailoring the *d*-band center of Ni by Cu for efficient and selective catalytic hydrogenation of furfural. *J. Catal.* **2020**, *383*, 172-180.
23. Warren, N. J.; Armes, S. P., Polymerization-induced self-assembly of block copolymer nano-objects via RAFT aqueous dispersion polymerization. *J. Am. Chem. Soc.* **2014**, *136*, 10174-10185.
24. Rae Cho, K.; Kim, Y.-Y.; Yang, P.; Cai, W.; Pan, H.; Kulak, A. N.; Lau, J. L.; Kulshreshtha, P.; Armes, S. P.; Meldrum, F. C.; De Yoreo, J. J., Direct observation of mineral-organic composite formation reveals occlusion mechanism. *Nat. Commun.* **2016**, *7*, 10187.
25. Hendley, C. T.; Fielding, L. A.; Jones, E. R.; Ryan, A. J.; Armes, S. P.; Estroff, L. A., Mechanistic Insights into Diblock Copolymer Nanoparticle-Crystal Interactions Revealed via in Situ Atomic Force Microscopy. *J. Am. Chem. Soc.* **2018**, *140*, 7936-7945.
26. Zhong, X.; Shtukenberg, A. G.; Hueckel, T.; Kahr, B.; Ward, M. D., Screw Dislocation Generation by Inclusions in Molecular Crystals. *Cryst. Growth & Des.* **2018**, *18*, 318-323.
27. Zhong, X.; Shtukenberg, A. G.; Liu, M.; Olson, I. A.; Weck, M.; Ward, M. D.; Kahr, B., Dislocation Generation by Microparticle Inclusions. *Cryst. Growth Des.* **2019**, *19*, 6649-6655.
28. Ning, Y.; Han, L.; Douverne, M.; Penfold, N. J. W.; Derry, M. J.; Meldrum, F. C.; Armes, S. P., What Dictates the Spatial Distribution of Nanoparticles within Calcite? *J. Am. Chem. Soc.* **2019**, *141*, 2481-2489.
29. Kim, Y. Y.; Semsarilar, M.; Carloni, J. D.; Cho, K. R.; Kulak, A. N.; Polishchuk, I.; Hendley IV, C. T.; Smeets, P. J.; Fielding, L. A.; Pokroy, B., Structure and properties of nanocomposites formed by the occlusion of block copolymer worms and vesicles within calcite crystals. *Adv. Funct. Mater.* **2016**, *26*, 1382-1392.
30. Kulak, A. N.; Semsarilar, M.; Kim, Y.-Y.; Ihli, J.; Fielding, L. A.; Cespedes, O.; Armes, S. P.; Meldrum, F. C., One-pot synthesis of an inorganic heterostructure: uniform occlusion of magnetite nanoparticles within calcite single crystals. *Chem. Sci.* **2014**, *5*, 738-743.
31. Kulak, A. N.; Yang, P.; Kim, Y.-Y.; Armes, S. P.; Meldrum, F. C., Colouring crystals with inorganic nanoparticles. *Chem. Commun.* **2014**, *50*, 67-69.

32. Ning, Y.; Fielding, L. A.; Nutter, J.; Kulak, A. N.; Meldrum, F. C.; Armes, S. P., Spatially Controlled Occlusion of Polymer - Stabilized Gold Nanoparticles within ZnO. *Angew. Chem. Int. Ed.* **2019**, *58*, 4302-4307.
33. Kim, Y.-Y.; Darkins, R.; Broad, A.; Kulak, A. N.; Holden, M. A.; Nahi, O.; Armes, S. P.; Tang, C. C.; Thompson, R. F.; Marin, F.; Duffy, D. M.; Meldrum, F. C., Hydroxyl-rich macromolecules enable the bio-inspired synthesis of single crystal nanocomposites. *Nat. Commun.* **2019**, *10*, 5682.
34. Magnabosco, G.; Polishchuk, I.; Palomba, F.; Rampazzo, E.; Prodi, L.; Aizenberg, J.; Pokroy, B.; Falini, G., Effect of Surface Chemistry on Incorporation of Nanoparticles within Calcite Single Crystals. *Cryst. Growth & Des.* **2019**, *19*, 4429-4435.
35. Ning, Y.; Fielding, L.; Andrews, T.; Growney, D.; Armes, S., Sulfate-based anionic diblock copolymer nanoparticles for efficient occlusion within zinc oxide. *Nanoscale* **2015**, *7*, 6691-6702.
36. Ning, Y.; Fielding, L. A.; Doncom, K. E.; Penfold, N. J.; Kulak, A. N.; Matsuoka, H.; Armes, S. P., Incorporating Diblock Copolymer Nanoparticles into Calcite Crystals: Do Anionic Carboxylate Groups Alone Ensure Efficient Occlusion? *ACS Macro Lett.* **2016**, *5*, 311-315.
37. Ning, Y.; Fielding, L. A.; Ratcliffe, L. P. D.; Wang, Y.-W.; Meldrum, F. C.; Armes, S. P., Occlusion of Sulfate-Based Diblock Copolymer Nanoparticles within Calcite: Effect of Varying the Surface Density of Anionic Stabilizer Chains. *J. Am. Chem. Soc.* **2016**, *138*, 11734-11742.
38. Ning, Y.; Han, L.; Derry, M. J.; Meldrum, F. C.; Armes, S. P., Model Anionic Block Copolymer Vesicles Provide Important Design Rules for Efficient Nanoparticle Occlusion within Calcite. *J. Am. Chem. Soc.* **2019**, *141*, 2557-2567.
39. Ning, Y.; Whitaker, D. J.; Mable, C. J.; Derry, M. J.; Penfold, N. J.; Kulak, A. N.; Green, D. C.; Meldrum, F. C.; Armes, S. P., Anionic block copolymer vesicles act as Trojan horses to enable efficient occlusion of guest species into host calcite crystals. *Chem. Sci.* **2018**, *9*, 8396-8401.
40. Ning, Y.; Meldrum, F. C.; Armes, S. P., Efficient occlusion of oil droplets within calcite crystals. *Chem. Sci.* **2019**, *10*, 8964-8972.
41. Chi, J.; Zhang, W.; Wang, L.; Putnis, C. V., Direct Observations of the Occlusion of Soil Organic Matter within Calcite. *Environ. Sci. Technol.* **2019**, *53*, 8097-8104.
42. Ihli, J.; Levenstein, M. A.; Kim, Y.-Y.; Wakonig, K.; Ning, Y.; Tatani, A.; Kulak, A. N.; Green, D. C.; Holler, M.; Armes, S. P.; Meldrum, F. C., Ptychographic X-ray tomography reveals additive zoning in nanocomposite single crystals. *Chem. Sci.* **2020**, *11*, 355-363.
43. Zhang, L.; Lu, Q.; Lv, X.; Shen, L.; Zhang, B.; An, Z., In Situ Cross-Linking as a Platform for the Synthesis of Triblock Copolymer Vesicles with Diverse Surface Chemistry and Enhanced Stability via RAFT Dispersion Polymerization. *Macromolecules* **2017**, *50*, 2165-2174.
44. Kim, Y.-Y.; Fielding, L. A.; Kulak, A. N.; Nahi, O.; Mercer, W.; Jones, E. R.; Armes, S. P.; Meldrum, F. C., Influence of the Structure of Block Copolymer Nanoparticles on the Growth of Calcium Carbonate. *Chem. Mater.* **2018**, *30*, 7091-7099.
45. Douverne, M.; Ning, Y.; Tatani, A.; Meldrum, F. C.; Armes, S. P., How Many Phosphoric Acid Units Are Required to Ensure Uniform Occlusion of Sterically Stabilized Nanoparticles within Calcite? *Angew. Chem. Int. Ed.* **2019**, *58*, 8692-8697.
46. Fielding, L. A.; Hendley IV, C. T.; Asenath-Smith, E.; Estroff, L. A.; Armes, S. P., Rationally designed anionic diblock copolymer worm gels are useful model systems for calcite occlusion studies. *Polym. Chem.* **2019**, *10*, 5131-5141.

47. Gorna, K.; Muñoz-Espí, R.; Gröhn, F.; Wegner, G., Bioinspired Mineralization of Inorganics from Aqueous Media Controlled by Synthetic Polymers. *Macromol. Biosci.* **2007**, *7*, 163–173.
48. Li, H.; Xin, H. L.; Muller, D. A.; Estroff, L. A., Visualizing the 3D internal structure of calcite single crystals grown in agarose hydrogels. *Science* **2009**, *326*, 1244-1247.
49. Liu, Y.; Yuan, W.; Shi, Y.; Chen, X.; Wang, Y.; Chen, H.; Li, H., Functionalizing Single Crystals: Incorporation of Nanoparticles Inside Gel - Grown Calcite Crystals. *Angew. Chem. Int.l Ed.* **2014**, *53*, 4127-4131.
50. Liu, Y.; Zang, H.; Wang, L.; Fu, W.; Yuan, W.; Wu, J.; Jin, X.; Han, J.; Wu, C.; Wang, Y., Nanoparticles incorporated inside single-crystals: enhanced fluorescent properties. *Chem. Mater.* **2016**, *28*, 7537-7543.